

DETAILED DAMAGE MECHANISMS ASSESSMENT IN COMPOSITE MATERIALS BY MEANS OF X-RAY TOMOGRAPHY

F. Sket^{1*}, A. Enfedaque², C. Alton³, S. Sadaba¹, J. Molina-Aldareguia¹, C. González^{1,2},
J. Llorca^{1,2}

¹IMDEA Materials Institute, C/ Profesor Aranguren s/n, Madrid, Spain.

²Polytechnical University of Madrid, E. T. S. de Ingenieros de Caminos, 28040-Madrid, Spain

³Michigan state University, East Lansing, MI, USA

*e-mail: Federico.sketch@imdea.org

Keywords: Carbon fibre reinforced composites, X-ray tomography, damage evolution.

Abstract

This research focused on the evaluation of damage formation on $\pm 45^\circ$ carbon fiber laminates subjected to tensile tests. The damage was evaluated by means of X-ray tomography. A high density of cracks developed during the plateau of the stress-strain curve and were qualitatively analyzed, showing that the inner plies eventually developed a higher crack concentration than the outer plies. Delamination started to occur in the outermost ply interface when the slope after the plateau of the stress-strain curve began to increase.

1. Introduction

Carbon fibre reinforced polymers (CFRP) are widely used in structural components due to their high specific mechanical properties. Although there have been extensive experimental and theoretical studies of the material behaviour under different load conditions, improved understanding in regard to damage evolution and eventual failure is still needed. CFRP can present several different damage mechanisms, i.e. fibre fracture, fibre kinking, fibre pull-out, fibres scissoring, matrix cracking, debonding at fibre-matrix interface, delamination, and the dominant one depends on the load and deformation conditions. Prediction of the type and amount of damage in these composites due to mechanical loads is of main importance and the models predicting the effect of damage in the non-linear response of polymeric composites present still discrepancies with respect to experimental data. Therefore, a deep understanding of the fracture and deformation mechanisms and correlation to the global loading geometry and local stress field is needed. Moreover, composite laminates contain plies with the fibers oriented along different directions and, even in the case of simple uniaxial deformation, the failure mechanisms indicated above may co-exist in the same laminate, with the additional mode of interply delamination. The interaction between all these failure mechanisms is an important factor to take into account and to some extent define the load-bearing capacity of a composite material. These damage processes are very sensitive to various factors such as multiaxial stress states [1–3], panel size [4–6], ply thickness and stacking sequence [4,6,7] and stress concentrations [5–7].

High resolution X-Ray Computed Tomography (XCT) is a technique specially well suited to visualize the damage mechanisms in fibre reinforced polymers since it combines several

advantages of more traditional techniques (i. e. ultrasound, acoustic emission, infrared thermography, X-ray radiography, SEM, TEM, confocal microscopy, fluorescent microscopy and TOM), namely, resolution below micrometer level, generation of 3D images, deep penetration into either transparent or opaque materials and simple sample preparation. Thus, in this work, XCT was used to assess the sequence of crack propagation into a $\pm 45^\circ$ epoxy/carbon fibre composite. For this purpose plain specimens were sequentially tensile tested up to five different displacements and further examined by XCT.

2. Materials and testing methods

Panels of $300 \times 300 \times 1.0 \text{ mm}^3$ were autoclave manufactured using unidirectional prepreps made from carbon fibers pre-impregnated with epoxy resin (Hexcel, UK). The stacking sequence was $[\pm 45^\circ]_{4s}$. The nominal fiber volume fraction after consolidation was 34% and the resulting thickness was 1.0mm.

Specimens of $200 \times 20 \times 1.0 \text{ mm}^3$ (length \times depth \times thickness) were machined from the laminates with the external plies at $+45^\circ$. The tensile mechanical tests were carried out in an electromechanical universal testing machine (Instron 3384) at constant cross-head speed of 0.6mm/min. A typical shear stress-shear strain curve is shown in Figure 1. Two specimens, named sample N°1 and N°2, were loaded up to different loads, marked with circles and squares in Figure 1.

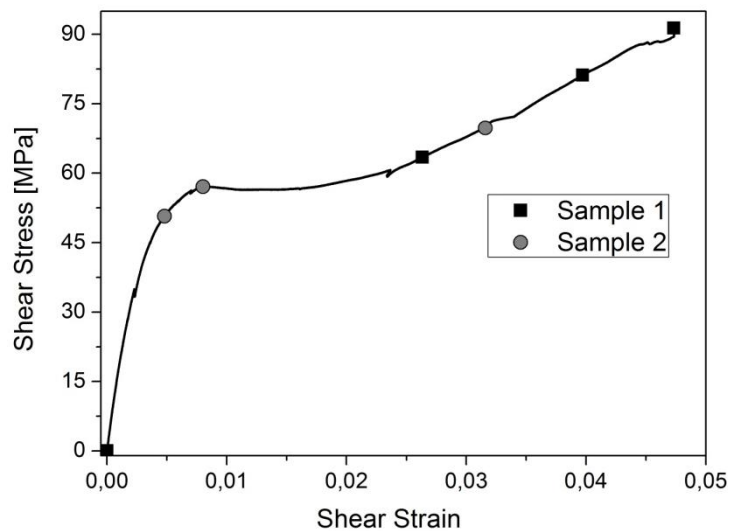


Figure 1. Shear stress-shear strain curve and the load points where the tomographic measurements were performed for each specimen

The specimen was immersed in a dye penetrant liquid once the desired load was reached, while the displacement was held constant. The dye penetrant technique was used to enhance the contrast between the cracks and the composite material in the tomograms. After this procedure the specimens were taken out from the tensile testing machine and scanned using an X-ray tomograph. Then, the sample was reloaded in the tensile machine to the next step and the procedure was repeated. The tomographic measurements were performed for all the loading stages (including the initial state) in the central part of the test coupons since no previous information of the final fracture location was available. The fracture occurred finally at one end of the samples close to the tab.

The different failure mechanisms and their spatial distribution were studied by XCT using a Nanotom 160NF system from Phoenix. The tomograms were collected at 90 kV and 100 μA

using a tungsten target. For each tomogram, 2000 radiographs were acquired with an exposure time of 750 ms. Tomogram resolution was set to approximately 10 $\mu\text{m}/\text{voxel}$. After the reconstruction of the volume, the damage in the reconstructed volumes were qualitatively analyzed.

3. Results and discussion

3.3 General observations

The inspection of the specimens tomographic data after loading up to the different loading states revealed that cracks start forming in the $\pm 45^\circ$ specimen, after the elastic limit was surpassed (at shear stresses between 50.7MPa and 57.1MPa). Short cracks emanating from the laminate edge were sparsely distributed along each ply and were observed on several plies in the sample loaded up to 57.1MPa.

Figure 2 shows an example of an external and inner ply of the samples N°2 at 69.8MPa. In the two set of samples investigated, the crack pattern was consistent with the loading conditions and showed a continuous increase in the number of cracks with the load. The crack pattern was clearly visible from a shear stress of 63.4MPa.

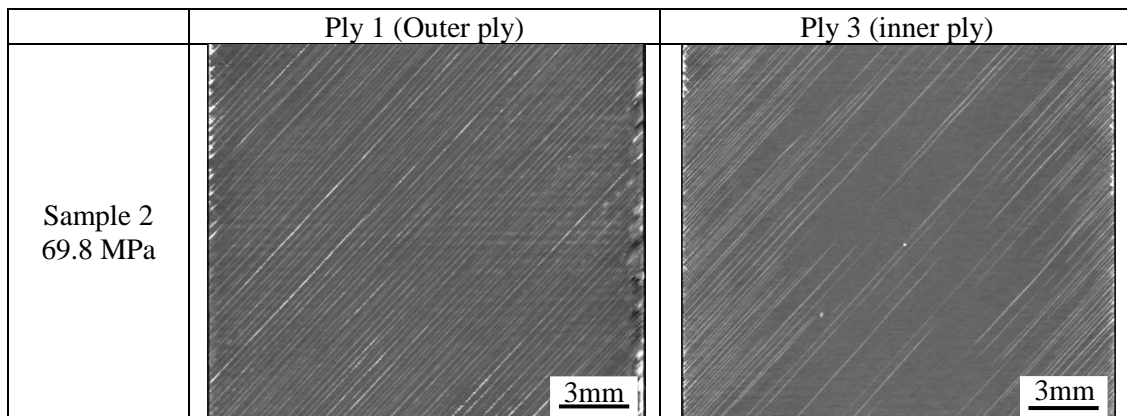


Figure 2. Crack pattern generated in an external (Ply1 – left column) and inner ply (Ply2 – right column) at shear loads of 69.8 MPa.

In both samples, the inner plies show the presence of cracks developing from both edges towards the center of the each lamina but not crossing the whole ply (right column of Figure 2). The cracks propagate towards the center of the ply with increasing load finally meeting at the center of the ply. This border effect leads to an inhomogeneous damage distribution in the direction of the laminate width for all plies.

Delamination between the plies was first observed at the edges at a shear stress of 63.4MPa. With increasing load, the delamination did not propagate from the edges to the interior of the laminate. However, small delaminations were generated at the intersection between cracks of consecutive plies along the whole interplay surface mainly in the outermost interface. This is shown in Figure 3(a) where a projection of the damage of two consecutive plies is observed. Just before fracture extensive edge delamination took place at the fracture position, and a tomographic scan was performed in this region too. The edge delamination which led to final fracture is shown in Figure 3(b).

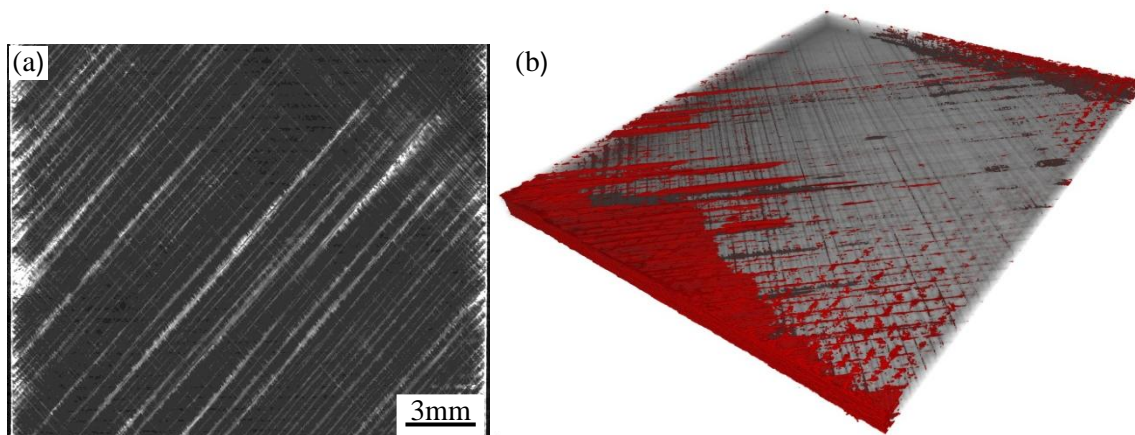


Figure 3. (a) Damage projection of plies 1 and 2 at a shear load of 91.3 MPa. Edge delamination do not propagate towards the middle of ply. Delamination at crack intersection is clearly visible between cracks at $+45^\circ$ and -45° . (b) Damage at the final fracture position at shear stress of 91.3 MPa.

Qualitatively it was observed that in the early stages of the loading procedure, the outermost plies showed a higher concentration of matrix cracks than the inner ones (Figure 2), and its concentration does not change much with the increase in load. In the inner plies, the situation is different and cracks formed during the whole stress-strain curve starting from the edge to the centre of the ply.

3. Conclusions

A qualitative analysis of the onset and evolution of damage in $\pm 45^\circ$ carbon fibre laminates was conducted by means of X-ray tomography. Damage started to be visible in the form of very short cracks emanating from the edges of the laminate at the limit of proportionality of the stress-strain curve. The crack pattern generated during the test is symmetric with respect to the center of the ply but its distribution is inhomogeneous, showing a higher concentration at the edges. Delamination at crack intersections start mainly at the outermost interfaces. Final fracture took place due to extensive localized edge delamination.

References

- [1] Hoppel CPR, Bogetti A, Gillespie JW. Literature review – effects of hydrostatic pressure on mechanical behavior of composite materials. *J Thermoplas Compos Mater* 1995;8:375–409.
- [2] Oguni K, Tan CY, Ravichandran G. Failure mode transition in unidirectional E-glass/vinylester composites under multiaxial compression. *J Compos Mater* 2000;34:2081–97.
- [3] Daniel IM, Luo JJ, Schubel PM, Werner BT. Interfiber/interlaminar failure of composites under multi-axial stress states. *Compos Sci Technol* 2009;69:764–71.
- [4] Wisnom MR, Khan B, Hallet SR. Size effects in unnotched tensile strength of unidirectional and quasi-isotropic carbon/epoxy composites. *Compos Struct* 2008;84:21–8.
- [5] Lee J, Soutis C. Measuring the notched compressive strength of composite laminates: specimen size effects. *Compos Sci Technol* 2008;68:2359–66.
- [6] Laffan MJ, Pinho ST, Robinson P, Iannucci L. Measurement of the in situ ply fracture toughness associated with mode I fibre tensile failure in FRP. Part II: size and lay-up effects. *Compos Sci Technol* 2010;70:614–21.
- [7] Wisnom MR, Hallet SR. The role of delamination in strength, failure mechanisms and hole size effect in open hole tensile tests on quasi-isotropic laminates. *Composites Part A* 2009;40:335–42.
- [8] Duda, R. O. and P. E. Hart, "Use of the Hough Transformation to Detect Lines and Curves in Pictures," *Comm. ACM*, Vol. 15, pp. 11–15 (January, 1972).